

*Dedicated to prof. dr. I. C. Popescu
on the occasion of his 70th anniversary*

EFFECT OF AMINES AS PROTON VECTORS ON CATALYTIC HYDROGEN EVOLUTION REACTION ON COPPER

**ÁGNES JAKAB^a, NICOLAE VASZILCSIN^{a*}, FLORICA MANEA^a,
MIRCEA DAN^a**

ABSTRACT. In this study, the catalytic effect of several organic amines on hydrogen evolution reaction (HER) was studied on copper. Kinetic parameters of electrode process were determined from Tafel polarization curves in order to obtain more information about the catalytic effect of the organic amines. The best electrocatalytic effect was reached in 0.5 M H₂SO₄ solution for N,N-dimethylaniline (DMA). A correlation between molecular parameters and electrocatalytic effect of amines have been performed. A larger dipole moment determined for N,N-dimethylanilinium (DMAH⁺) showed that the orientation of these molecules are more favorable ordered on the electrode surface. Also, electrochemical impedance spectroscopy (EIS) technique was used to assess quantitatively the DMA effect over the electrochemical parameters for HER on copper. A significant enhancement of charge transfer rate was noticed with DMA concentration and temperature increasing. In addition, the adsorption behavior of DMA on copper surface followed the Langmuir adsorption isotherm. The low negative values of the standard Gibbs free energy of adsorption ΔG_{ads} at different temperature suggested a physical sorption. The value of the activation energy determined for 10⁻³ M DMA was 37% lower than that determined in its absence. A direct involving of DMA in HER mechanism on the copper as proton carrier from bulk to the solution/metal interface was found.

Keywords: *proton carrier, electrocatalytic effect, hydrogen evolution reaction, Tafel plots, EIS*

^a Politehnica University of Timisoara, Faculty of Industrial Chemistry and Environmental Engineering, V. Párvan. No. 6, 300223 Timisoara, Romania.

* Corresponding author: nicolae.vaszilcsin@upt.ro

INTRODUCTION

It is well known that hydrogen can play an important role as energy carrier in the possible scenario for the future, with socio-economic benefits and positive environmental impact [1,2]. Hydrogen can be produced by a large number of processes, *i.e.*, thermochemical [3-5], electrochemical [4-9], photochemical [10-13], photocatalytic [14,15] and photo-electrochemical [16-18], having as a primary energy source a wide range of resources.

Among the above-mentioned processes, the electrochemical procedure based on the water electrolysis exhibits many advantages, such as: high purity, simple process, environmental friendliness and plenty of sources. However, the researchers are continuously motivated to find solutions for two major problems during electrolysis, related to the high energy consumption and the low gas evolution. To overcome these problems, most of research studies are focused on new electrode materials and strategies for improving the production process efficiency involving also, new electrolytic system [19].

Currently, cathodes based on platinum metals offer the best performance for catalytic enhancement of the hydrogen evolution reaction (HER). From an economic point of view, use of Pt-type catalysts present an obstacle to hydrogen energy economy, due to their high cost and low-abundance. For this reason, it is crucial to develop inexpensive advanced HER catalyst materials characterized by high activity and stability. Recent studies have been reported the high catalytic effect of molybdenum sulfide based catalysts for HER [20-26]. In few reports, researchers used carbon fibers as HER electrode materials modified with Pt nanoparticle/MoS₂ nanosheets characterized by low loading of Pt and thus, a higher electrocatalytic activity was obtained [27]. Metal alloys [28] and transition metal carbides (WC, Mo₂C, TaC, NbC) [29] have also used as potential electrocatalysts for HER. *In-situ* adding catalytic compounds into electrolyte to enhance gas evolution reaction was less approached, although it is promising due to the low cost and the simple operation. Kaninski et al. [30] added in electrolyte the mixture of Na-molybdate and tris(ethylenediamine) Co(III)chloride as ionic activator to catalyze HER. In this case, energy saving was about 10% in comparison with blank electrolyte solution.

Another very promising way to enhance HER on different metal electrodes is the addition of organic amines as proton vectors in electrolyte, which facilitate the transport of protons from bulk solution to the interface. In recent papers, the catalytic effect of various organic amines, *i.e.*, benzylamine, m-toluidine, aniline, 4-chloroaniline and methylamine towards HER was studied on different metal electrodes. The performed studies showed that the protonated form of amines act as proton carriers, accelerating the hydrogen evolution reaction [31-34].

The aim of this study was to investigate the catalytic effect of aniline (A), N,N-diethylaniline (DEA), N-ethylaniline (EA), N-methylaniline (MA), N,N-dimethylaniline (DMA), o-toluidine (oTO), m-toluidine (mTO) and p-toluidine (pTO) over HER on copper electrode in 0.5 M H₂SO₄ at different temperatures using Tafel polarization curves and electrochemical impedance spectroscopy (EIS) technique. Experiments were carried out at higher current densities, similar with those applied in commercial water electrolyzers, in contrast with results reported by Vaduva et al [33,34]. The adsorption features of amines on the cathode surface were studied based on Langmuir isotherm model.

RESULTS AND DISCUSSION

Based on previous studies regarding catalytic effect of amines on the hydrogen evolution reaction at copper [34], several organic amines with aromatic substituents have been investigated as catalysts in 0.5 M H₂SO₄ solution at copper electrode. Linear voltammetry curves were recorded from -0.5 to -1 V vs. Ag/AgCl on copper at 10 mVs⁻¹. Figure 1 presents the polarization curves for HER on copper in 0.5 M H₂SO₄ solution in the absence and the presence of various organic amines, *i.e.*, aniline (A), N,N-diethylaniline (DEA), N-ethylaniline (EA), N-methylaniline (MA), N,N-dimethylaniline (DMA), o-toluidine (oTO), m-toluidine (mTO) and p-toluidine (pTO).

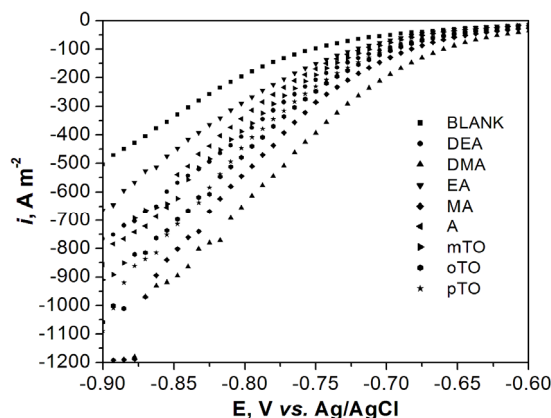


Figure 1. Linear voltammograms recorded on copper electrode in 0.5 M H₂SO₄ solution at 298 K; concentration of amines: 10⁻³ M, scan rate: 10 mVs⁻¹.

The above-presented linear polarization curves show that the current density increased in the presence of amines. The most significant electrocatalytic effect is observed in the presence of N,N-dimethylaniline (DMA) in relation to shifting the hydrogen evolution overpotential to less

negative potential value. Thus, in the presence of 10^{-3} M DMA in 0.5 M H_2SO_4 solution at 298 K, the current density of $500 A \cdot m^{-2}$ is reached at -0.75 V vs. Ag/AgCl in comparison with -0.9 V vs. Ag/AgCl for blank solution. In order to obtain more information about the catalytic effect of organic amines, kinetic parameters, e.g., Tafel slope (b), exchange current density (i_0) and cathodic transfer coefficient ($1-\alpha$), were determined from Tafel polarization curves. Two important parameters i_0 and b obtained by fitting the linear relationship between $\log(i)$ and η , are the criterions for the assessment of the catalytic activity of the catalysts. The higher exchange current and the smaller Tafel slope informed about the better catalytic performance of the catalyst. The obtained experimental results are gathered in Table 1, and it can be noticed that the best electrocatalytic effect was reached for DMA ($i_0=0.181 A \cdot m^{-2}$, $b=-138 mV \cdot dec^{-1}$) and DEA ($i_0=0.180 A \cdot m^{-2}$, $b=-159 mV \cdot dec^{-1}$).

Table 1. Kinetic parameters for HER in 0.5 M H_2SO_4 solution in the presence of different organic amines at 298 K and electronic characteristics of protonated amines.

Amine, 10^3 [M]	$-b$ [$mV \cdot dec^{-1}$]	$1-\alpha$	i_0 [$A \cdot m^{-2}$]	Molecular coverage [\AA^2] [35]	Dipole moment [D] [35]	LUMO [eV] [35]	HOMO [eV] [35]
DEAH ⁺	159	0.37	0.180	71.5	3.25	-0.009	-0.483
DMAH ⁺	138	0.43	0.181	58.5	5.30	-0.017	-0.489
EAH ⁺	149	0.39	0.084	51.1	4.85	-0.020	-0.489
MAH ⁺	143	0.41	0.117	45.0	6.32	-0.025	-0.493
AH ⁺	149	0.39	0.095	39.4	7.46	-0.032	-0.500
mTOH ⁺	138	0.43	0.054	44.4	8.32	-0.024	-0.483
oTOH ⁺	136	0.43	0.068	40.2	6.92	-0.027	-0.485
pTOH ⁺	142	0.41	0.090	40.5	8.85	-0.027	-0.488

It is well-known that the catalytic effect of the amines largely depends on their molecular characteristics [33]. The catalytic activity of the amine is due to a free electron pair present on the nitrogen atom and is dependent upon the availability of this electron pair for complexation [36]. Energy level of HOMO characterizes the ability of chemical entities to interact as electron donor, while energy level of LUMO is a descriptor of the electron acceptor properties [37]. Hence, DEAH⁺ and DMAH⁺ molecules with the lowest LUMO energy values (-0.009 eV, respectively -0.017 eV) are more able to accept electron than other molecules with higher LUMO energy values. This descriptor can be used to characterize adsorption properties of protonated amines. Despite the fact that DEAH⁺ is characterized by LUMO energy value lower than that of DMAH⁺, a modest catalytic effect was observed for DEA in comparison with DMA. This fact can be explained by the largest groups on the nitrogen atom that should increase steric hindrance and thus, for DEAH⁺ it is difficult to remove the proton that is masked by ethyl groups. As a consequence, methyl groups tend to

push electrons toward the nitrogen increasing the accessibility of the free electron pair, while ethyl groups tend to withdraw electrons, diminishing accessibility, thus reducing catalytic activity. Furthermore, the coverage area of DMAH⁺ (58.5 Å²) is smaller than that of DEAH⁺ (71.5 Å²), which allows the adsorption of a higher number of DMA molecules on the cathode surface. Under these conditions, a local concentration of hydronium ion at the electrode/solution interface is higher and as consequence, a higher exchange current density [32]. On the other hand, a larger dipole moment for DMAH⁺ (5.30 D) means that the orientation of these dipoles on the electrode surface are more ordered than of DEAH⁺ dipoles. This is another reason why a larger number of DMAH⁺ molecules will be able to adsorb on the electrode surface, favoring exchange current density increasing.

Based on above-presented results, DMA was selected for further experiments as catalyst for HER in 0.5 M H₂SO₄ solution. The critical operating parameters in the kinetics of HER are the temperature and the concentration of amine catalyst. Cathodic polarization experiments were performed at 298, 308, 318, 328 K, using different concentrations of DMA (10⁻⁶, 10⁻⁵, 10⁻⁴, 10⁻³ M). Figure 2 shows as examples Tafel plots for the HER on copper electrode in absence and presence of DMA at different temperatures.

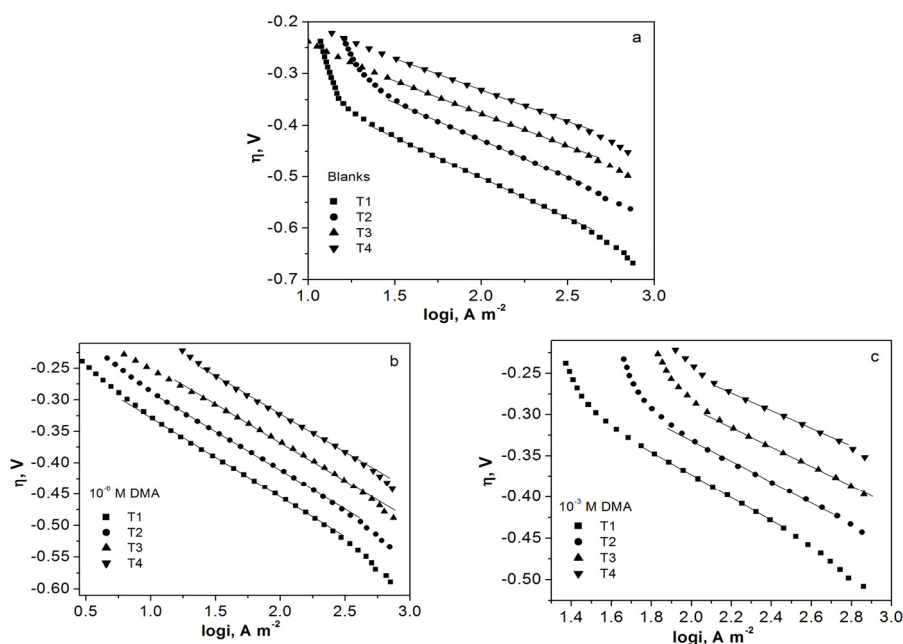


Figure 2. Tafel plots for HER on copper electrode in blank 0.5 M H₂SO₄ solution (a) and in the presence of different concentrations of DMA: 10⁻⁶ M (b), 10⁻³ M (c); at different temperatures: T₁ = 298 K; T₂ = 308 K; T₃ = 318 K; T₄ = 328 K.

Based on Tafel plots, the kinetic parameters for the HER at different temperatures and concentrations of DMA were determined and summarized in Table 2.

It can be noticed, that in the presence of different concentrations of DMA a larger electrocatalytic activity was obtained than in its absence, according to the comparison of the exchange current density i_0 . For example, the addition of 10^{-3} M DMA leads to increasing the exchange current density of about 12 times as compared to the blank solution at 298 K. In addition, the Tafel slope obtained for all studied cases was about $-120 \text{ mV}\cdot\text{dec}^{-1}$ approaching to the theoretical value of $-118 \text{ mV}\cdot\text{dec}^{-1}$, showing that the HER in the absence and presence of DMA proceeded based on a Volmer-Heyrovsky mechanism. According to Flecher [38], this fact indicate that the formation of $(\text{H}\cdot)_{\text{ads}}$ is slow and the destruction of $(\text{H}\cdot)_{\text{ads}}$ is fast.

Table 2. Kinetic parameters for HER on copper electrode in the absence and presence of DMA at different temperatures

C_{DMA} [M]	T [K]	$-b$ [mV dec ⁻¹]	$1-\alpha$	i_0 [A·m ⁻²]
0	298	132	0.45	0.015
	308	128	0.48	0.037
	318	126	0.50	0.103
	328	121	0.54	0.194
10^{-6}	298	126	0.47	0.024
	308	124	0.49	0.045
	318	122	0.52	0.094
	328	120	0.54	0.214
10^{-5}	298	126	0.47	0.039
	308	121	0.50	0.054
	318	115	0.55	0.102
	328	115	0.57	0.222
10^{-4}	298	135	0.44	0.109
	308	132	0.46	0.191
	318	119	0.53	0.220
	328	116	0.56	0.378
10^{-3}	298	138	0.43	0.181
	308	126	0.48	0.232
	318	118	0.53	0.347
	328	107	0.61	0.461

Also, the apparent activation energies for HER charge transfer process were calculated from the slope of the linear dependence $\log i_0=f(T^{-1})$ according to Eq.(1) [33]:

$$E_a = -2.303R \frac{\partial(\lg i_0)}{\partial(T^{-1})} \quad (1)$$

Figure 3 shows the Arrhenius plots in the absence and presence of DMA at different temperatures. The values of the activation energy obtained based on Figure 3 were $69.14 \text{ kJ}\cdot\text{mol}^{-1}$ in the absence of DMA, $58.83 \text{ kJ}\cdot\text{mol}^{-1}$ for 10^{-6} M DMA, $46.01 \text{ kJ}\cdot\text{mol}^{-1}$ for 10^{-5} M DMA, $30.89 \text{ kJ}\cdot\text{mol}^{-1}$ for 10^{-4} M DMA and respective, $25.6 \text{ kJ}\cdot\text{mol}^{-1}$ for 10^{-3} M DMA. It is obviously that the charge transfer rate is favored by increasing DMA concentration due to the activation energy decreased at higher DMA concentration. This aspect informed that even if DMA adsorption on the cathode surface is a prerequisite conditions to enhance HER, removing of adsorbed DMA from the cathode surface did not require an extra energy, which indicates a weak adsorption effect.

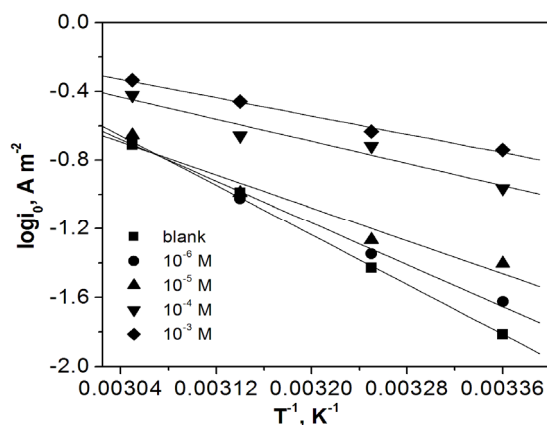
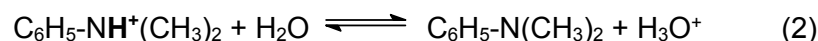


Figure 3. Arrhenius plots for HER in $0.5 \text{ M H}_2\text{SO}_4$ and in the presence of different concentrations of DMA.

DMA action on HER kinetics is rather complex, since the catalytic activity depends not only on concentration, temperature and molecular properties, but also on the surface coverage degree related to amine adsorption on the electrode-electrolyte interface [34]. Organic amines are very slightly soluble in water, protonation of these amine molecules potentially increase solubility and ion balance in water is given by Eq.(2):



N,N-dimethylaniline is protonated in sulphuric acid forming aryl-ammonium ions [34], which are preferentially oriented with the ammonium group to the metal surface and the catalytic effect is due to their strong adsorption.

In order to assess quantitatively the electrochemical parameters for HER, electrochemical impedance spectroscopy (EIS) technique was used as a very useful tool. Based on polarization curve results, EIS spectra were recorded on copper electrode at the overpotential of -0.4 V vs. Ag/AgCl in 0.5 M

H₂SO₄ supporting electrolyte without and respective, with various concentrations of DMA and different temperatures ranged between 298 and 328 K. As example, in Figure 4 are shown EIS results expressed as Nyquist and Bode plots determined for the temperature of 308 K and various DMA concentrations.

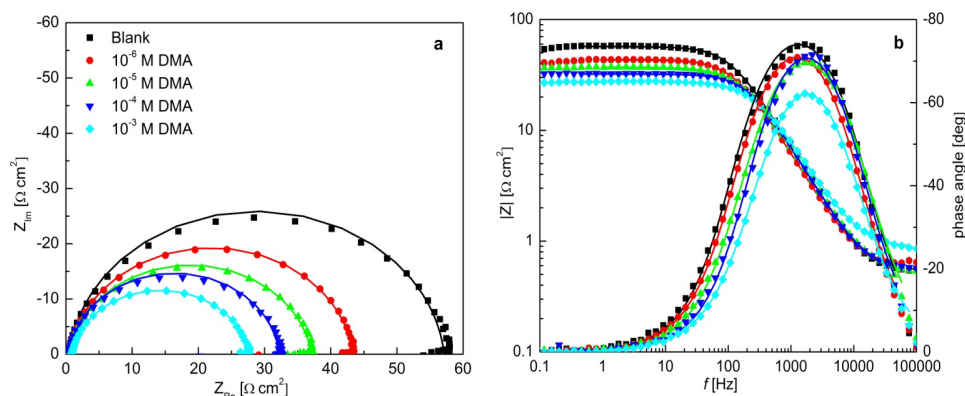


Figure 4. Experimental Nyquist (a) and Bode (b) plots at overpotential of -0.4 V and $T = 308$ K for HER on copper in 0.5 M H₂SO₄ with different concentrations of DMA. Symbols are experimental points and continuous line are simulated by the CNLS fitting according to the electrical equivalent circuit.

Nyquist spectra showed a slightly suppressed semicircle that indicates about an electron transfer limiting process, which is assessed by charge transfer resistance (R_{ct}). It is obviously that increasing DMA concentration led to decreasing R_{ct} that can be easily evaluated as semicircle width. R_{ct} decreasing in the presence of DMA indicates the enhancement of the charge transfer process rate. From Bode spectrum, it can be noticed the existence of one time constant phase for both supporting electrolyte and DMA presence, which confirm that DMA presence did not change the HER mechanism. Also, the thermal effect is to accelerate the charge transfer process (see Table 3).

For a precise description of the HER process, the experimental impedance data were fitted to the electrical equivalent circuit (EEC) given in Figure 5, using a complex non-linear least squares (CNLS) procedure.

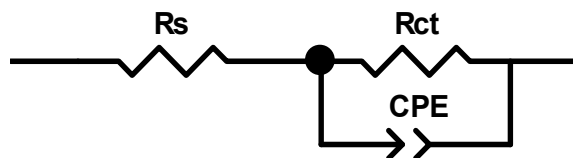


Figure 5. Equivalent electrical circuit for modelling the HER on copper electrode in acid medium.

The electrical equivalent circuit consists of a resistance R_s in series with a parallel connection of the charge transfer resistance R_{ct} and a constant phase element (CPE). The resistance R_s includes the uncompensated solution resistance. The ideal capacitor characterized by double layer capacity is usually replaced by a constant phase element (CPE) since it describes more accurately the behaviour of real electrochemical systems, the CPE impedance is described by the Eq.(3) [33]:

$$Z_{CPE} = 1/T(j\omega)^n \quad (3)$$

where T is a parameter proportional with double layer capacity, n is an exponent ranged between 0 and 1, which describes CPE angle.

The results of the fitting are shown as continuous line in Figure 4 and the corresponding values of the circuit elements are given in Table 3.

Table 3. EEC parameter values for HER at overpotential of -0.4 V on copper in 0.5 M H₂SO₄ with different concentrations of DMA.

C [M]	T [K]	R_s [Ω cm ²]	$T \cdot 10^5$ [F cm ⁻² s ⁿ⁻¹]	n	R_{ct} [Ω cm ²]	$C_{dl} \cdot 10^5$ [F cm ⁻²]	Chi ²
0	298	0.32	6.19	0.86	158	1.01	2.0·10 ⁻³
	308	0.53	3.70	0.91	56.6	1.27	3.8·10 ⁻³
	318	0.67	3.55	0.92	23.0	1.41	1.0·10 ⁻³
	328	0.99	3.84	0.92	12.8	1.60	3.1·10 ⁻⁴
10 ⁻⁶	298	0.77	4.53	0.88	136	1.10	2.5·10 ⁻³
	308	0.59	4.21	0.92	42.8	1.67	5.1·10 ⁻⁴
	318	0.91	4.01	0.93	19.6	1.87	9.1·10 ⁻⁴
	328	0.91	4.38	0.92	8.57	1.83	9.9·10 ⁻⁴
10 ⁻⁵	298	0.64	5.07	0.89	105	1.45	2.6·10 ⁻³
	308	0.52	4.56	0.92	36.6	1.83	1.2·10 ⁻³
	318	0.75	4.05	0.94	13.3	2.10	4.4·10 ⁻⁴
	328	0.46	3.91	0.95	6.08	2.21	7.7·10 ⁻⁴
10 ⁻⁴	298	0.39	5.48	0.90	75.2	1.66	3.2·10 ⁻³
	308	0.57	3.69	0.95	31.6	2.15	2.7·10 ⁻³
	318	0.88	4.42	0.94	9.39	2.33	8.8·10 ⁻⁴
	328	0.74	3.93	0.96	4.91	2.61	2.4·10 ⁻³
0 ⁻³	298	0.54	5.95	0.91	44.6	2.14	2.9·10 ⁻³
	308	0.88	4.46	0.94	26.8	2.34	7.5·10 ⁻⁴
	318	0.63	4.94	0.95	6.68	2.76	2.2·10 ⁻³
	328	0.67	4.25	0.97	3.45	3.09	1.1·10 ⁻³

Based on the results gathered in Table 3, it can be noticed the catalytic effect of DMA over hydrogen evolution process, which is confirmed by decreasing the value of charge transfer resistance with increasing the DMA concentration and the temperature. Also, increased values of double layer capacity indicated DMA adsorption on internal Helmholtz layer, which is favored by higher DMA concentration and temperature.

Therefore, the degree of surface coverage (θ) can be calculated from the charge transfer resistance as the following Eq.(4) [39]:

$$\theta = 1 - \frac{R_{ct}}{R_{ct}^*} \times 100 \quad (4)$$

where R_{ct} is the charge transfer resistance for catalyzed solution and R_{ct}^* is the charge transfer resistance for blank solution. Basic information on the interaction between the surface of copper and amine can be determined from Langmuir adsorption isotherm.

The degree of surface coverage (θ) for different concentrations of the amine (C_{DMA}) has been evaluated. The data were tested graphically to determine a suitable adsorption isotherm. The straight line with linear correlation coefficient (R^2) is almost equal to 1.0, was obtained on plotting C_{DMA}/θ vs. C_{DMA} at all studied different temperatures as shown in Figure 6, suggesting that adsorption of the amine on the copper surface obeys the Langmuir adsorption isotherm. According to the Langmuir adsorption isotherm, the surface coverage is related to DMA concentration by Eq.(5) [40]:

$$\frac{C_{DMA}}{\theta} = \frac{1}{K_{ads}} + C_{DMA} \quad (5)$$

where K_{ads} is the equilibrium constant.

The intercept allows the calculation of the equilibrium constant K_{ads} being related to the standard free energy adsorption (ΔG_{ads}) as shown in the following Eq.(6) [41]:

$$K_{ads} = \frac{1}{55.5} \exp\left(-\frac{\Delta G_{ads}^0}{RT}\right) \quad (6)$$

where 55.5 is the concentration of water in solution expressed in mole.

The obtained linear regressions and correlation coefficients are given in Table 4.

Table 4. Thermodynamic parameters for the adsorption of DMA on copper in 0.5 M H₂SO₄ at different temperatures

T [K]	Linear regression	R^2	K_{ads} [M ⁻¹]	$-\Delta G_{ads}$ [kJ·mol ⁻¹]
298	$y = 4.58 \cdot 10^{-5} + 1.09x$	0.999	1.09	10.17
308	$y = 9.80 \cdot 10^{-5} + 1.18x$	0.999	1.18	10.71
318	$y = 4.86 \cdot 10^{-4} + 1.34x$	0.998	1.34	11.40
328	$y = 3.08 \cdot 10^{-4} + 1.56x$	0.999	1.56	12.17

The negative values of standard free energy obtained for different temperatures, indicate the spontaneous adsorption of DMA, due to the electrostatic interaction between the protonated molecules of amine and the charge metal surface (physical sorption).

In this case, the values of ΔG_{ads} less than $-20 \text{ kJ}\cdot\text{mol}^{-1}$ are consistent with the physical adsorption. The values of ΔG_{ads} around $-40 \text{ kJ}\cdot\text{mol}^{-1}$ or higher suggest a chemisorption.

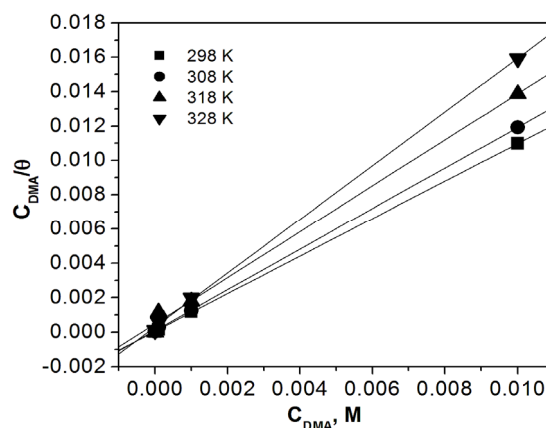


Figure 6. Langmuir's adsorption plots for DMA on the copper electrode surface in 0.5 M H_2SO_4 at different temperatures.

EIS results corroborated with polarization curve results proved direct involving of DMA in HER mechanism on the copper electrode as proton carrier from bulk to the solution/metal interface.

CONCLUSIONS

In this study, the catalytic effect of several organic amines on hydrogen evolution reaction (HER) was studied on copper electrode in 0.5 M H_2SO_4 at different temperatures. In order to obtain more information about catalytic effect of organic amines, kinetic parameters were determined from Tafel polarization curves, e.g., Tafel slope (b), exchange current density (i_0). Based on these kinetic parameters, it was found that N,N-dimethylaniline (DMA) exhibited the best electrocatalytic effect.

The aspects regarding mechanism elucidation were discussed based on the molecular parameters of protonated amines. A larger dipole moment determined for N,N-dimethylanilinium (DMAH^+) showed that the orientation of these molecules are more favorable ordered on the electrode surface.

The value of the activation energy determined for 10^{-3} M DMA was 37% lower than that obtained in the absence of DMA. Also, electrochemical impedance spectroscopy (EIS) results showed a significant favorable effect of DMA concentration increasing on the rate of the charge transfer process for HER expressed by charge transfer resistance (R_{ct}). A great reducing of R_{ct} value was noticed with DMA concentration and temperature increasing.

A possible adsorption of DMA on internal Helmholtz layer of solution/electrode interface was found. In addition, the adsorption behavior of DMA on copper surface was studied by Langmuir adsorption isotherm model that fitted well the experimental data. The low negative values of the standard Gibbs free energy of adsorption at different temperature suggested a physical sorption of DMA on the copper electrode.

DMA acted as a proton carrier from bulk to the solution/metal interface and exhibited the catalytic activity towards the hydrogen evolution reaction.

EXPERIMENTAL SECTION

The chemicals used for this study *i.e.*, sulphuric acid (H_2SO_4), aniline ($C_6H_5NH_2$), N,N-diethylaniline ($(C_2H_5)_2NC_6H_5$), N-ethylaniline ($C_6H_5NHC_2H_5$), N-methylaniline ($C_6H_5NHCH_3$), N,N-dimethylaniline ($C_8H_{11}N$), o-toluidine ($CH_3C_6H_4NH_2$), m-toluidine ($CH_3C_6H_4NH_2$) and p-toluidine ($CH_3C_6H_4NH_2$) (analytical grade) were purchased from Merck Company (Germany). The distilled water was used for all experiments. The experimental set-up consisted of a conventional three-electrode single-chamber glass cell and a PAR 2273 potentiostat/galvanostat equipped with PowerCV specific module for linear voltammetry. The potentiostat was connected with a platinum sieve counter electrode, Ag/AgCl reference electrode and a copper working electrode with 0.5 cm^2 surface area. All electrode potentials are reported with respect to Ag/AgCl. The working electrode surface was polished before each experiment with a soft abrasive paper and rinsed with distilled water. Luggin capillary was positioned very close to the electrode surface in order to avoid the ohmic drop through the electrolyte solution. Thermo Scientific DC 10 - thermostat was used to control the solution temperature in the range of 298-328 K ($\pm 0.1\text{K}$). All solutions were deoxygenated thoroughly by purging with high purity nitrogen gas. Details of the calculation of the reversible potential E_{rev} (vs. the normal hydrogen electrode) for the HER in 0.5 M H_2SO_4 solution have been reported in our previous published paper [31].

EIS measurements were carried out using the FRA module of Biologic SP150, in the frequency range from 0.01 Hz to 100 kHz and AC voltage amplitude of 10 mV. For each spectrum 60 points were collected,

with a logarithmic distribution of 10 points per decade. The experimental electrochemical impedance data were fitted based on the electrical equivalent circuit by CNLS Levenberg – Marquardt procedure using ZView – Scribner Associates Inc. software.

ACKNOWLEDGMENTS

„This work was partially supported by the strategic grant POSDRU/159/1.5/S/137070 (2014) of the Ministry of National Education, Romania, co-financed by the European Social Fund – Investing in People, within the Sectoral Operational Programme Human Resources Development 2007-2013.”

REFERENCES

1. I. Dincer, C. Acar, *International Journal of Hydrogen Energy*, **2014**, 1.
2. S. Sharma, S.K. Ghoshal, *Renewable Sustainable and Energy Reviews*, **2015**, 43, 1151.
3. Y. Zhang, R. Wang, X. Lin, Z. Wang, J. Liu, J. Zhou, K. Cen, *Applied Catalysis B: Environmental*, **2015**, 166–167, 413.
4. T. Kawada, H. Yamashita, Q. Zheng, M. Machida, *International Journal of Hydrogen Energy*, **2014**, 39(35), 20646.
5. A.C. Tizzoni, N. Corsaro, C. D'Ottavi, S. Licoccia, S. Sau, P. Tarquini, *International Journal of Hydrogen Energy*, **2015**, 40(11), 4065.
6. J.A. Allen, G. Rowe, J.T. Hinkley, S.W. Donne, *International Journal of Hydrogen Energy*, **2014**, 39(22), 11376.
7. B. Pierozynski, *International Journal of Electrochemical Science*, **2011**, 6, 63.
8. F. Safizadeh, E. Ghali, G. Houlachi, *International Journal of Hydrogen Energy*, **2015**, 40, 256.
9. A. Survila, S. Kanapeckaitė, J. Pileckienė, J. Budiene, *International Journal of Electrochemistry*, **2011**, 9.
10. A.A. Ismail, D.W. Bahnemann, *Solar Energy Materials and Solar Cells*, **2014**, 128, 85.
11. C. Zamfirescu, I. Dincer, G.F. Naterer, *International Journal of Hydrogen Energy*, **2012**, 37(12), 9537.
12. W. Yao, X. Song, C. Huang, Q. Xu, Q. Wu, *Catalysis Today*, **2013**, 199, 42.
13. Z. Wang, R.R. Roberts, G.F. Naterer, K.S. Gabriel, *International Journal of Hydrogen Energy*, **2012**, 37(21), 16287.
14. D. Praveen Kumar, N. Lakshmana Reddy, M. Mamatha Kumari, B. Srinivas, V. Durga Kumari, B. Sreedhar, V. Roddatis, O. Bondarchuk, M. Karthik, B. Neppolian, M.V. Shankar, *Solar Energy Materials and Solar Cells*, **2015**, 136, 157.
15. W. Zhang, S. Wang, J. Li, X. Yang, *Catalysis Communications*, **2015**, 59, 189.

16. J. Ji, L. Guo, Q. Li, F. Wang, Z. Li, J. Liu, Y. Jia, *International Journal of Hydrogen Energy*, **2015**, 40(10), 3813.
17. T. Zhu, M.N. Chong, *Nano Energy*, **2015**, 12, 347.
18. D. Sharma, A. Verma, V.R. Satsangi, R. Shrivastav, S. Dass, *International Journal of Hydrogen Energy*, **2014**, 39(9), 4189.
19. M. Wang, Z. Wang, X. Gong, Z. Guo, *Renewable and Sustainable Energy Reviews*, **2014**, 29, 573.
20. D. Wang, Z. Pan, Z. Wu, Z. Wang, Z. Liu, *Journal of Power Sources*, **2014**, 264, 229.
21. S.S.J. Aravind, M. Costa, V. Pereira, A. Mugweru, K. Ramanujachary, T.D. Vaden, *International Journal of Hydrogen Energy*, **2014**, 39(22), 11528.
22. J. Ji, L. Guo, Q. Li, F. Wang, Z. Li, J. Liu, Y. Jia, *International Journal of Hydrogen Energy*, **2015**, 40(10), 3813.
23. D. Wang, Z. Wang, C. Wang, P. Zhou, Z. Wu, Z. Liu, *Electrochemistry Communications*, **2013**, 34, 219.
24. B.B. Li, S.Z. Qiao, X.R. Zheng, X.J. Yang, Z.D. Cui, S.L. Zhu, Z.Y. Li, Y.Q. Liang, *Journal of Power Sources*, **2015**, 284, 68.
25. X. Xia, Z. Zheng, Y. Zhang, X. Zhao, C. Wang, *International Journal of Hydrogen Energy*, **2014**, 39(18), 9638.
26. A.W. Jeremiasse, J. Bergsma, J.M. Kleijn, M. Saakes, C.J.N. Buisman, M.C. Stuart, H.V.M. Hamelers, *International Journal of Hydrogen Energy*, **2011**, 36(17), 10482.
27. D. Hou, W. Zhou, X. Liu, K. Zhou, J. Xie, G. Li, S. Chen, *Electrochimica Acta*, **2015**, 166, 26.
28. A.W. Jeremiasse, J. Bergsma, J.M. Kleijn, M. Saakes, C.J.N. Buisman, M.C. Stuart, H.V.M. Hamelers, *International Journal of Hydrogen Energy*, **2011**, 36(17), 10482.
29. S. Meyer, A.V. Nikiforov, I.M. Petrushina, K. Köhler, E. Christensen, J.O. Jensen, N.J. Bjerrum, *International Journal of Hydrogen Energy*, **2015**, 40(7), 2905.
30. M.P.M. Kaninski, V.M. Nikolic, T.N. Potkonjak, B.R. Simonovic, N.I. Potkonjak, *Applied Catalysis A: General*, **2007**, 321, 93.
31. R. Cretu, A. Kellenberger, N. Vaszilcsin, *International Journal of Hydrogen Energy*, **2013**, 38, 11685.
32. R. Cretu, A. Kellenberger, M. Medeleanu, N. Vaszilcsin, *International Journal of Electrochemical Science*, **2014**, 9, 4465.
33. C.C. Vaduva, N. Vaszilcsin, A. Kellenberger, M. Medeleanu, *International Journal of Hydrogen Energy*, **2011**, 36(12), 6994.
34. C.C. Vaduva, N. Vaszilcsin, A. Kellenberger, *International Journal of Hydrogen Energy*, **2012**, 37, 12089.
35. C.C. Vaduva, "PhD. Thesis", Ed. Politehnica, Timisoara, **2013**.
36. M. Szycher, "Szycher's Handbook of Polyurethanes", CRC-Press, USA, **2013**.
37. C. Reichardt, "Solvents and Solvent Effects in Organic Chemistry", WILEY-VCH, Germany, **2003**.
38. S. Fletcher, *Journal of Solid State Electrochemistry*, **2009**, 13, 537.
39. M.N. El-Haddad, *Carbohydrate Polymers*, **2014**, 112, 595.
40. N. Abdulwali, F. Mohammed et al., *International Journal of Electrochemical Science*, **2014**, 9, 6402.
41. A.M. Al-Bonayan, *International Journal of Electrochemical Science*, **2015**, 10, 589.